Advances in Water Resources 127 (2019) 280–290

Contents lists available at ScienceDirect

Advances in Water Resources

journal homepage: www.elsevier.com/locate/advwatres

# A simplified MEV formulation to model extremes emerging from multiple nonstationary underlying processes

Francesco Marra*, Davide Zoccatelli, Moshe Armon, Efrat Morin

*Fredy & Nadine Herrmann Institute of Earth Sciences, Hebrew University of Jerusalem, E.J. Safra Campus - Givat Ram, Jerusalem 9190401, Israel*

ARTICLE INFO

*Keywords:*
Extreme value analysis
Metastatistical extreme value
Nonstationary processes
Climate change
Daily precipitation

ABSTRACT

This paper presents a Simplified Metastatistical Extreme Value formulation (SMEV) able to model hydro-meteorological extremes emerging from multiple underlying processes. The formulation explicitly includes the average intensity and probability of occurrence of the processes allowing to parsimoniously model changes in these quantities to quantify changes in the probability of occurrence of extremes. SMEV allows (a) frequency analyses of extremes emerging from multiple underlying processes and (b) computationally efficient analyses of the sensitivity of extreme quantiles to changes in the characteristics of the underlying processes; moreover, (c) it provides a robust framework for explanatory models, nonstationary frequency analyses, and climate projections.

The methodology is applied to daily precipitation data from long recording stations in the eastern Mediterranean, using Weibull distributions to model daily precipitation amounts generated by two classes of synoptic systems. At-site application of SMEV provides spatially consistent estimates of extreme quantiles, in line with regional GEV estimates and generally characterized by reduced uncertainties. The sensitivity of extreme quantiles to changes and uncertainty in the intensity and yearly occurrences of events generated by different synoptic classes is examined, and an application of SMEV for the projection of future extremes is provided.

## 1. Introduction

Quantifying hydro-meteorological extremes in a changing climate is crucial to build resilience and plan water resources management and hydrological design. Frequency analysis consists in the identification of a cumulative distribution function whose upper tail represents the probability of exceedance of high (extreme) values of the stochastic process of interest. This is generally done assuming no temporal dependence (stationarity) in the statistical description of the process, but evidences of climate change (e.g., Hall et al., 2014; Fisher and Knutti, 2016) call for the development of models able to cope with changing (nonstationary) conditions. The term "nonstationary" refers to a time-indexed process subject to temporal changes in its statistical description. In this study, in particular, we will address deterministic temporal changes (Koutsoyiannis and Montanari, 2015) in both (a) the probability of occurrence of the process and (b) the parameters describing its cumulative distribution function.

A review of earlier studies on nonstationary frequency analysis is provided by Khaliq et al. (2006). Recent modelling efforts of future hydro-meteorological extremes are based on two main approaches. The first one consists of detecting trends in the process of interest, from either observations or climate models, and extrapolating such trends using extreme value formulations (e.g., Villarini et al., 2009; Westra et al., 2013; Cheng and AghaKouchak, 2014; Agilan and Umamahesh, 2017). The second approach relies on the identification and quantification of causative relations between the process of interest and other explanatory variables (e.g., Hardwick Jones et al., 2010; Berg et al., 2013; Lepore et al., 2015; Serago and Vogel, 2018) with the intent of gathering information on the future characteristics of extreme processes from the changes in the explanatory variables. A relevant example is the scaling relation between temperature and extreme precipitation, object of numerous studies in recent years (e.g., Westra et al., 2014; Dobrinski et al., 2016; Wasko et al., 2016). Nonetheless, these approaches are subject to assumptions, uncertainties, and overfitting issues that prevent the current models from being fully trusted (Morin, 2011; Serinaldi and Kilsby, 2015; Serinaldi and Kilsby, 2018; Serinaldi et al., 2018).

A common background to these analyses is extreme value theory: assuming independence and identical distribution of the examined process (i/id assumption) and large enough ($n \to \infty$) number of occurrences of the process in each year (asymptotic assumption), the distribution of extremes may only converge to known distribution classes (Fischer and Tippett, 1928; Gnedenko, 1943). However, hydro-meteorological extremes may arise from multiple underlying processes (e.g., convective versus stratiform precipitation, just to mention a simple example), so that the i/id assumption is often not met. Moreover, the number of independent events in a year is far from being infinite, violating the

* Corresponding author.
*E-mail address:* marra.francesco@mail.huji.ac.il (F. Marra).

https://doi.org/10.1016/j.advwatres.2019.04.002
Received 19 October 2018; Received in revised form 31 March 2019; Accepted 3 April 2019
Available online 3 April 2019
0309-1708/

asymptotic assumption. To overcome the violation of the i/id assumption, some studies included seasonal separation of the events (Willems, 2000; Fisher, 2018; Iliopoulou et al., 2018) or (multi-)variate models considering external explanatory variables in the formulation (Sun et al., 2014; Pineda and Willems, 2018). These approaches allow to include external information in the perspective of future climate modeling and were shown to improve the estimation of extreme quantiles for the studied cases. This, however requires the estimation of a large number of parameters, a complicated effort that can give rise to important uncertainties due to the limited data availability and, when interested in future projections, to the inaccuracy characterizing extremes in climate models (e.g., Kendon et al., 2017; Meresa and Romanowicz, 2017).

The Metastatistical Extreme Value (MEV) framework, proposed by Marani and Ignaccolo (2015), relaxes the asymptotic assumption and allows the identification of the parameters from a largely increased data sample (Zorzetto et al., 2016). Moreover, it has the potential to model extremes arising from multiple distributions, thus providing potential to overcome both of the above highlighted issues (Marani and Ignaccolo, 2015; Marra et al., 2018). Explicitly nonstationary formulations of the MEV approach as well as formulations including extremes arising from multiple types of events, however, are not available so far.

The objective of this study is to introduce a Simplified MEV formulation (SMEV) in which inter-annual variations are neglected and extremes are described as functions of the average properties of multiple underlying processes. Specific objectives are: (a) expanding the MEV framework to extremes emerging from multiple underlying processes; (b) introducing the SMEV formulation; (c) applying SMEV to daily precipitation records in the eastern Mediterranean; and (d) providing some example applications to sensitivity analyses and climate projections.

The paper is organized as follows. Section 2 provides the analytical formulation of SMEV. Section 3 describes the application of SMEV to frequency analysis of daily precipitation in the eastern Mediterranean, and to sensitivity analyses and future projections. Section 4 discusses the results of the study, and Section 5 summarizes the main conclusions.

## 2. Formulation

### 2.1. MEV formulation for extremes emerging from multiple underlying processes

The MEV approach (Marani and Ignaccolo, 2015) treats as stochastic variables both the parameters defining the cumulative distribution function of the process magnitudes observed during a given year, and the number of times a process (hereinafter termed “ordinary event” or simply “event”) is observed in each of the years. Denoting with $M$ the number of available years, $n_j$ the number of events observed during the $j^{\text{th}}$ year, and $F(\cdot)$ the cumulative distribution function of the distribution class describing the ordinary event magnitude $x$, described by $L$ parameters $\boldsymbol{\theta}_j = (\theta_j^1, \ldots, \theta_j^L)$, the MEV cumulative distribution function can be written as a sample average of the cumulative distribution functions observed during the sampled years:

$$MEV(x) = \frac{1}{M} \cdot \sum_{j=1}^{M} \left[ F\left(x; \boldsymbol{\theta}_j\right) \right]^{n_j}. \tag{1}$$

The reader interested in additional details is referred to Marani and Ignaccolo (2015) and Zorzetto et al. (2016). The MEV approach relaxes the asymptotic assumption of extreme value theory and makes use of all the available data to fit the distribution parameters. This drastically decreases the fitting uncertainty with respect to classic extreme value theory, which only exploits a small subset of the data, i.e. the annual maxima or the peaks exceeding a high threshold. Analyses of the performance of the methodology with respect to classic extreme value analyses can be found in Marani and Ignaccolo (2015), Zorzetto et al. (2016), and Marra et al. (2018). On the other hand, the formulation in Eq. (1) requires prior knowledge of the distribution class describing the underlying ordinary events, and assumes identical distribution of the ordinary events within each year. Whilst information on the former can be gained mining the available data, identical distribution of the ordinary events within each year can still represent strong requirement: the presence of extremes emerging from multiple distributions needs to be considered to accurately use the method (Marra et al., 2018).

Relaxing the assumption of identical distribution within each year, multiple types of ordinary events can be included in the framework. Let’s consider $S$ types of ordinary events and denote with $F_i(\cdot)$ the distribution class describing the $i^{\text{th}}$ type of ordinary events, parametrized at the $j^{\text{th}}$ year by $\boldsymbol{\theta}_{i,j}$. If the $i^{\text{th}}$ type of ordinary events is sampled $n_{i,j}$ times during the $j^{\text{th}}$ year (so that $n_j = \sum_{i=1}^{S} n_{i,j}$), the MEV cumulative distribution function can be written as:

$$MEV(x) = \frac{1}{M} \cdot \sum_{j=1}^{M} \left[ \prod_{i=1}^{S} \left[ F_i\left(x; \boldsymbol{\theta}_{i,j}\right) \right]^{n_{i,j}} \right]. \tag{2}$$

This formulation allows to explicitly include different types of ordinary events in the frequency analysis of extreme events, thus permitting to quantify the probability of occurrence of extremes caused by multiple underlying processes. In practice, one needs to match each ordinary event to the corresponding type, fit each $F_i(\cdot)$ to the $n_{i,j}$ ordinary events of the $i^{\text{th}}$ type occurred during the $j^{\text{th}}$ year, and then use Eq. (2) to derive the compound cumulative distribution function describing the resulting extremes. This, however, requires to identify a large number of parameters ($M \cdot \sum_{i=1}^{S} 1 + L_i$), a problematic task in presence of limited data samples, e.g. for situations in which only a limited number of events is observed each year (Marra et al., 2018), which is even emphasized when the ordinary events are divided into multiple types.

### 2.2. Simplified MEV (SMEV) formulation

Allowing inter-annual variability of the parameters describing the ordinary events distribution, the MEV framework allows to derive accurate frequency analyses able to represent the period over which data is analyzed and implicitly accounting for possible nonstationary conditions. However, this theoretical advantage needs to be balanced with the practical need to estimate parameters from limited number of yearly ordinary events. In fact, parameter estimation uncertainty may lead to biased estimates of the quantiles of interest, particularly important in situations in which only a limited number of events per year is observed (Marra et al., 2018). In fact, it should be noted that the inter-annual variations of the ordinary events distribution parameters reported by previous studies (e.g., Marani and Ignaccolo, 2015) are co-caused by three effects: (i) inter-annual variations of the characteristics of the ordinary events; (ii) parameter estimation uncertainty; and (iii) varying proportions in the occurrence of different types of ordinary events, in case the identical distribution assumption within each year is not verified. In order to be correctly represented, inter-annual variations of the parameters need to be larger than the uncertainty introduced by the other effects. Fig. S1 shows the uncertainty related to the parameter estimation method for a typical case, which gives a sense of the minimum detectable inter-annual variations of the parameters as a function of the number of ordinary events per year.

In this section, we introduce a simplified formulation in which the inter-annual variability is neglected both in the ordinary events distributions (i.e., assuming identical distribution of the ordinary events of each type – identical distribution assumption) and in their number of yearly occurrences (mean probability of occurrence approximation) for each event type. The identical distribution assumption should not come as a surprise, as adopted by all classic methods based on extreme value theory and already suggested as a way to decrease the parameter estimation uncertainty by Marani and Ignaccolo (2015) and Marra et al. (2018). Moreover, it allows parsimonious $L_i$-parameter expressions for the ordinary events. Note that, when multiple types of ordinary events are considered, the assumption should be intended as identical distribution of the events of each type during the years: different event types will still

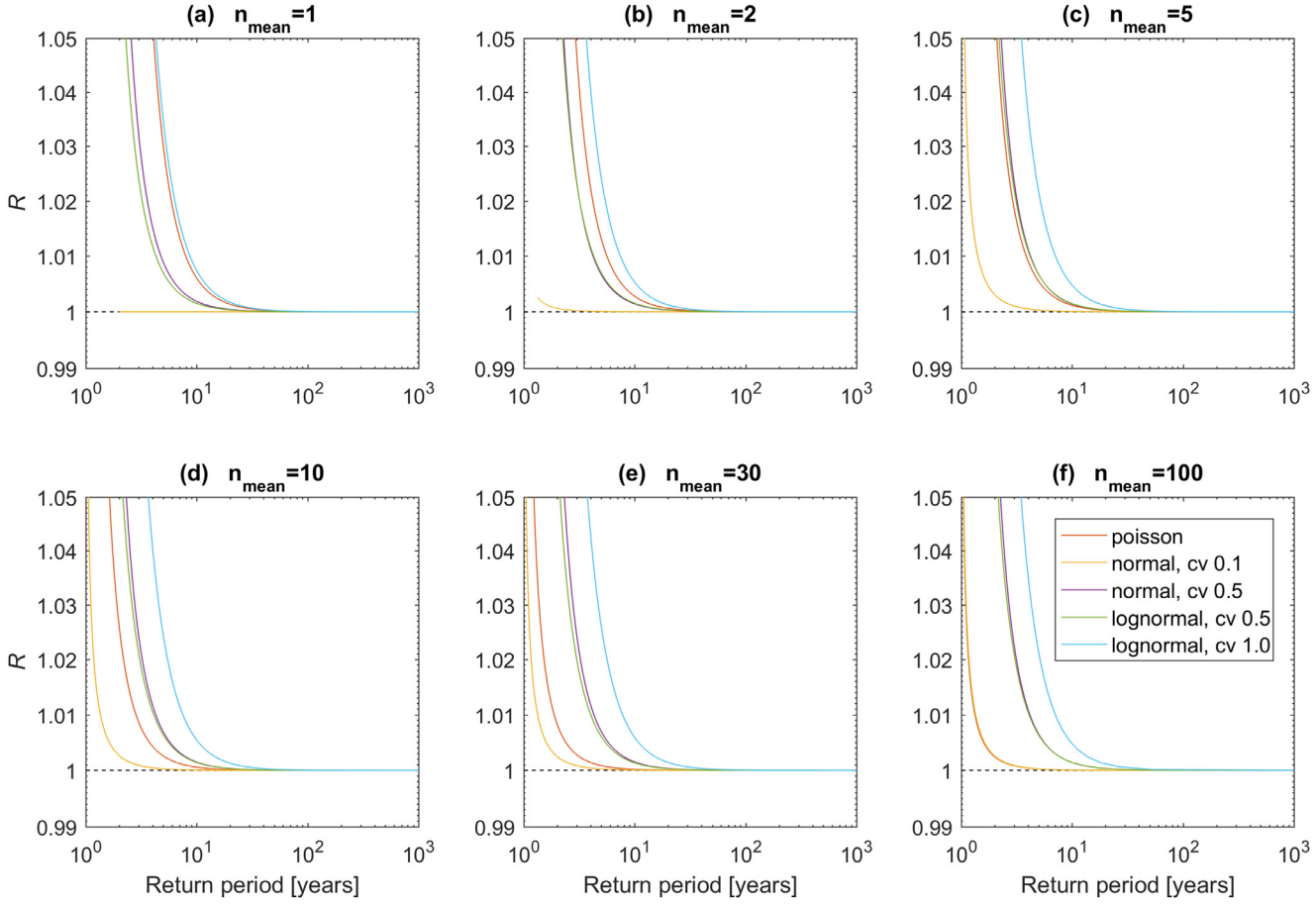


**Fig. 1.** Magnitude of the term $R$ plotted as a function of the return period. Note that, under identical distribution assumption, this plot is independent from the distribution of the ordinary events $F(\cdot)$. The term $R$ contains all the information on the inter-annual variability of the number of events per year $n_j$ (defined Eq. (4)). The figure displays a set of distributions of $n_j$ characterized by varying dispersions and skewness. The term $R$ goes quickly to 1 showing that, when interested in extremes, the inter-annual variability of $n_j$ becomes negligible. See also Fig. S1.

be described by different distributions. The mean probability of occurrence approximation of the traditional MEV expression will be analyzed more in detail in the following.

The identical distribution assumption allows to factorize the terms of Eq. (2) in which the mean number of ordinary events per year appears in the exponent:

$$MEV(x) = \prod_{i=1}^{S} \left[F_i(x;\theta_i)\right]^{n_i} \cdot \frac{1}{M} \sum_{j=1}^{M} \left[\prod_{i=1}^{S} \left[F_i(x;\theta_i)\right]^{\delta_{i,j}}\right] \tag{3}$$

where $n_i = \frac{1}{M} \cdot \sum_{j=1}^{M} n_{i,j}$ is the mean number of $i^{\text{th}}$ type ordinary events occurring in a year, $\delta_{i,j} = n_{i,j} - n_i$ are the deviations of the yearly values $n_{i,j}$ from the mean $n_i$, and the term

$$R = \frac{1}{M} \sum_{j=1}^{M} \left[\prod_{i=1}^{S} \left[F_i(x;\theta_i)\right]^{\delta_{i,j}}\right] \tag{4}$$

contains all the information on the inter-annual variability of $n_{i,j}$. In addition, the identical distribution assumption allows to analytically express $R$ as a function of the compound probability $MEV(x)$ without dependence on the distributions $F_i(\cdot)$ and on their parameters (as shown in Fig. 1). Taking the limit case $F(\cdot) \to 1$ (i.e. analyzing extremes), the term $R$ goes to 1 quickly, becoming negligible for the estimation of return periods exceeding ~10 years for a wide variety of distributions of $n_{i,j}$ (Fig. 1, Fig. S2).

The Simplified MEV (SMEV) formulation, in which any inter-annual variability is neglected, is thus written as:

$$SMEV(x) = \prod_{i=1}^{S} \left[F_i(x;\theta_i)\right]^{n_i} \tag{5}$$

The SMEV formulation drastically reduces the number of parameters (to $\sum_{i=1}^{S} 1 + L_i$), and allows a direct interpretation of their meaning: for each event type, $L_i$ parameters describe the ordinary events intensity ($\theta_i$), and one parameter is related to their probability of occurrence ($n_i$). Such parameters have clear physical meaning and can be extracted relatively easily from observation, or from either global/regional circulation models, climate projections and reanalyses (e.g., Tabari and Willems, 2018), which increasingly represent the sources of available information. When past data records are analyzed, Eq. (5) provides information for the average conditions observed during the study period, while it assumes a prognostic meaning for conditions in which the values of the parameters can be inferred, simulated, or projected. Noteworthy, the term $R$ can be computed for any distribution of the number of yearly occurrences $n_{i,j}$ (again, with no dependence on the $F_i(\cdot)$ and on their parameters when expressed as a function of the estimated return period) and, in case its impact is considered important, used to adjust the SMEV estimates.

Under nonstationary conditions, both the intensity of the ordinary evens (i.e., the $\theta_i$ parameters if one, reasonably, assumes no changes in the functional forms $F_i(\cdot)$) and their yearly probability of occurrence (i.e., $n_i$), can be expressed as a function of time, yielding the SMEV

nonstationary formulation:

$$SMEV(x,t) = \prod_{i=1}^{S} \left[F_i\left(x;\theta_i(t)\right)\right]^{n_i(t)} \quad (6)$$

In the following we explore the merit of describing changing extremes by incorporating a temporal dependence in (a) the intensity characteristics of different types of ordinary events ($\theta_i(t)$), and (b) their individual probability of occurrence ($n_i(t)$). Changes in any of the parameters in Eq. (6) can be easily modeled, including simultaneous changes of intensity and occurrence of different types of events.

## 3. Application

In this section, we show an application of SMEV for (a) modeling extremes emerging from multiple underlying processes, (b) quantifying the sensitivity of extreme quantiles to potential changes in the intensity and probability of occurrence of the individual type of ordinary event, and (c) providing an illustrative example of future projections based on simple trends in the characteristics of the ordinary events.

We focus on daily precipitation, which is among the most widely investigated hydro-meteorological processes. The approach, however, applies to any process for which the characteristics of the upper tail can be described by the ordinary events. Precipitation is caused by the condensation of atmospheric water vapor due to the lifting and cooling of air masses, which can be driven by different synoptic, meteorological and local conditions that, in turn, generate different precipitation patterns (e.g., Hirschboeck, 1987; Yarnal, 1993). A classic example is the distinct characteristics of convective and stratiform precipitation, but, as in this application, different types of events can be identified depending on the climatology of the region of interest.

### 3.1. Study area and data

The eastern Mediterranean region, focus of this application, is characterized by unique climatic conditions in which the Mediterranean climate characterizing the coastal region abruptly changes to semiarid and arid in the space of few tens of kilometers (Fig. 2). Precipitation occurs in the winter months and transitional seasons, with almost no rainfall from mid-June to mid-September. Precipitation is usually brought by Mediterranean lows, with minor, but still relevant, contributions from the active Red Sea trough, a synoptic system that may bring humidity from the Red Sea (de Vries et al., 2013). On rare occasions, other synoptic systems bring extreme precipitation to the region (e.g., Armon et al., 2018). We focus on two classes of synoptic systems known to display distinct precipitation characteristics (e.g., Dayan and Morin, 2006; Belachsen et al., 2017; Armon et al., 2018): (a) Mediterranean lows (hereinafter "Type 1–Lows", including both Cyprus lows and Lows to the East in the classification by Belachsen et al. (2017)), and (b) active Red Sea troughs and other synoptic systems (hereinafter "Type 2–Other"). Observations and model projections show substantial changes in the precipitation

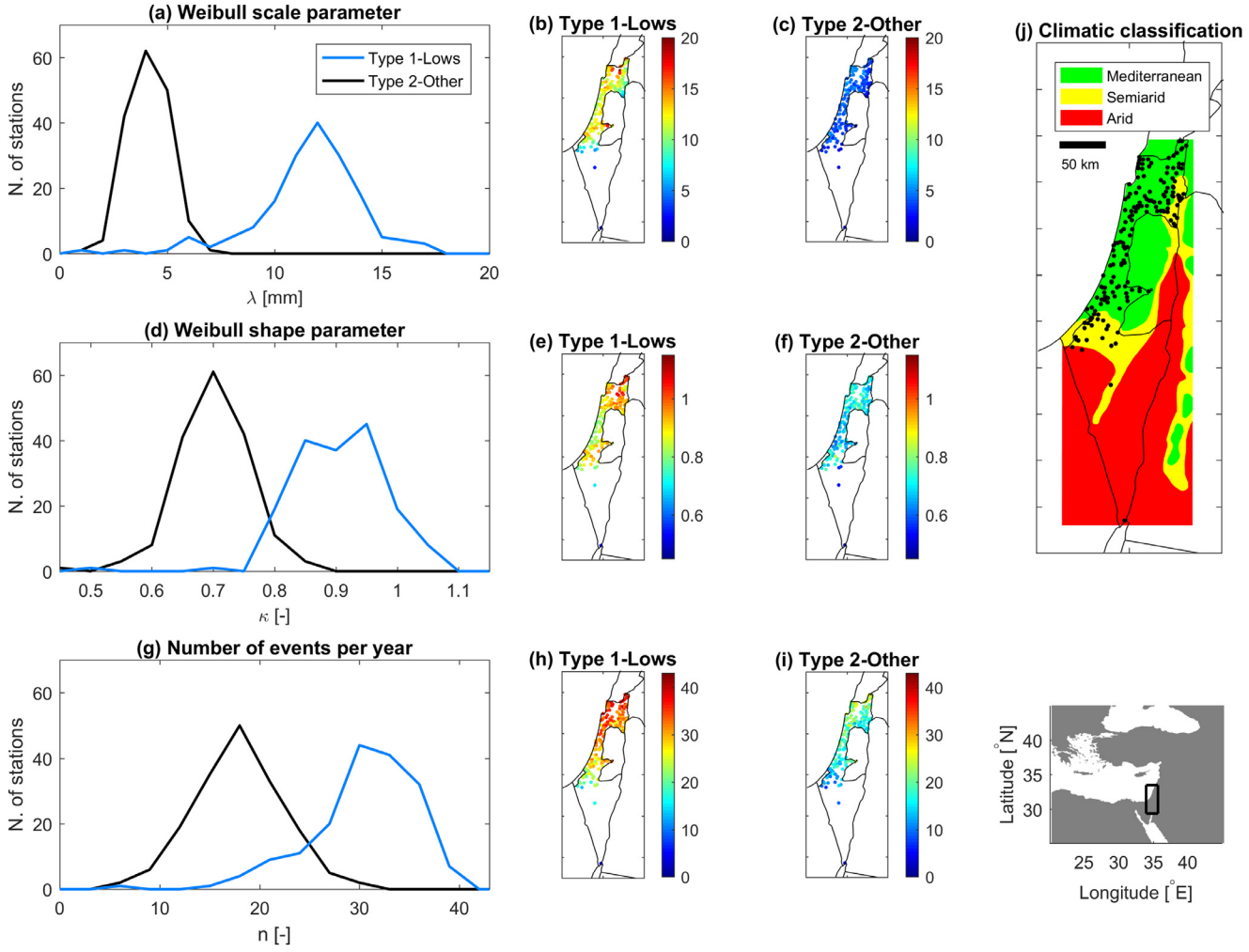


**Fig. 2.** Parameters of the Weibull distributions describing the two synoptic types: (a-c) scale parameter; (d-f) shape parameter; (g-i) number of events per year. (j) Climatic classification of the area (Atlas of Israel, 1970), location of the stations, and location of the area within the eastern Mediterranean region.

climatology of the region in response to changes in the frequency of occurrence of these synoptic systems, making the topic of high relevance (e.g., Alpert et al., 2002; Ziv et al., 2010; Peleg et al., 2015a; Hochman et al., 2018b).

A large dataset of daily precipitation made available by the Israel Meteorological Service, including data from 170 stations with at least 60-year record in the period 1948–2018, is used (Fig. 2). For each station, ordinary events are defined as non-zero (i.e., above or equal to 0.1 mm) daily precipitation amounts (Zorzetto et al., 2016), and labeled according to the generating synoptic class derived from the classification by Alpert et al., (2004) and Hochman et al., (2018a).

### 3.2. SMEV formulation for daily precipitation

Following the reasoning by Wilson and Tuomi (2005) and previous findings (Marani and Ignaccolo, 2015; Zorzetto et al., 2016; Marra et al., 2018; Papalexiou et al., 2018), ordinary events are modeled using a Weibull distribution (Weibull, 1951), whose cumulative distribution function can be written as:

$$W(x;\lambda,\kappa) = 1 - e^{-\left(\frac{x}{\lambda}\right)^{\kappa}}, \tag{7}$$

where $\lambda \in ]0, +\infty[$ and $\kappa \in ]0, +\infty[$ are the scale and shape parameters, respectively. Larger scale parameters are associated to larger magnitude of the average events, and larger shape parameters to lighter upper tail of the distribution. We use the SMEV formulation, assuming the presence of multiple processes underlying the daily precipitation extremes, i.e. multiple event types. This leads to a three-parameter description ($\lambda_i$, $\kappa_i$, $n_i$) of each event type $i$, with two parameters describing the events intensity ($\lambda_i$, $\kappa_i$) and one representing the number of yearly occurrences ($n_i$):

$$SMEV(x) = \prod_{i=1}^{S} \left[W\left(x;\lambda_i,\kappa_i\right)\right]^{n_i} = \prod_{i=1}^{S} \left[1 - e^{-\left(\frac{x}{\lambda_i}\right)^{\kappa_i}}\right]^{n_i}, \tag{8}$$

a description that can be easily made nonstationary including temporal dependence in the parameters of interest.

### 3.3. Parameters estimation methods

#### 3.3.1. Weibull parameters fit

Application of the MEV can be sensitive to the lower tail of the ordinary events distribution (Marra et al., 2018). In fact, low-intensity ordinary events may diverge from the distribution describing the upper tail (e.g., Fig. 3) due to the finite precision of the measuring instruments, to the subjective definition of rainy/non-rainy day, and to the presence of different physical processes. Thus, the lower tail needs to be disregarded in the computation of the parameters describing the upper tail of the compound distribution. Following Marani and Ignaccolo (2015), we propose to left-censor the observations (i.e., to exclude from the fit values below a given threshold) to avoid these issues. Given the high variability of precipitation regimes worldwide and the need to treat different types of ordinary events potentially characterized by different magnitudes, we propose to left-censor the data using a case-dependent threshold (e.g., a given quantile of the ordinary events) instead of the fixed 10 mm threshold proposed by Marani and Ignaccolo (2015). Sensitivity analyses based on the datasets used in this study showed that left-censoring values between the 55th quantile and the 80th quantile all provide virtually indistinguishable results (Fig. S2) while left-censoring using different thresholds may cause biases in the estimated parameters due to either the inclusion of low-intensity events, non-representative of the upper tail, or to the use of an insufficient data sample from the upper tail itself (Fig. 3). In this study, we treat the two types of ordinary events independently, and chose a threshold equal to the 75th quantile of the ordinary events. The remaining 25% of the data points are observed to well represent the upper-tail in all the stations examined in this study, and still allow to use a sufficiently large data sample (at least 75 data points, but usually more than 400, are available in the examined dataset). Weibull parameters are then derived using the least-squares method (Marani and Ignaccolo, 2015) on the remaining data points (Fig. 3), and included in the SMEV formulation in Eq. (8).

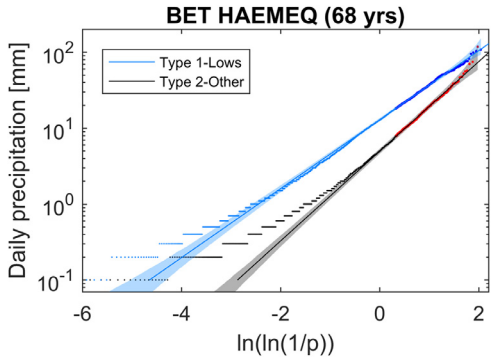


**Fig. 3.** Weibull fit of 2 types of ordinary events (i.e., Type 1–Lows and Type 2–Other) for an example station. The station name and record length are given in the figure title. Points represent all the ordinary events, large points with different colour the events used for the Weibull fit (top 25%), solid lines the Weibull distribution fitting the data, and shaded areas the 90% Weibull sampling uncertainty, obtained from 2000 random draws from the distribution fitting the data. On the x-axis, $p$ represents the exceedance probability. Notice the deviation of low intensity events from the distribution characterizing the upper tail.

#### 3.3.2. Regional frequency analysis

Regional frequency analysis is used to indirectly test the quality of the at-site SMEV analyses. Homogeneous groups of stations are identified based on climatic classification and geographic proximity. Homogeneity of the regions is ensured with the test based on the coefficient of L-variation recommended by Hosking and Wallis (1997). A regional frequency analysis based on L-moments is then adopted and the GEV distribution is used to describe the regional growth curves of the annual maxima series normalized over their mean values (Hosking and Wallis, 1997). Regional GEV frequency curves for each station are then computed.

#### 3.3.3. Quantification of uncertainty

Uncertainty related to the frequency analyses is quantified using bootstrap with replacement of $M$ random years out of the $M$ years in the full records (1000 repetitions; Overeem et al., 2008). The method allows to quantify the uncertainty related to the use of a particular methodology (here SMEV and regional GEV) considering the statistical characteristics and the length of the available data record.

### 3.4. Extreme daily precipitation in the eastern Mediterranean

The proposed formulation is applied to the frequency analysis of extreme daily precipitation amounts arising from two classes of synoptic patterns in the eastern Mediterranean. Fig. 2 shows very distinct parameter sets to describe the two classes, implying that (a) the identical distribution assumption cannot be regarded as accurate, and (b) the adopted synoptic classification is meaningful. In general, Type 1–Lows are characterized by larger scale parameter (i.e., larger average daily precipitation amounts), larger shape parameter (i.e., less skewed distribution, lighter-tailed extremes), and larger number of yearly occurrences. These observations confirm well-known features of the synoptic systems (Dayan and Morin, 2006; Armon et al., 2018), and their separate integration in the framework allows to correctly quantify their relative impact on extremes.

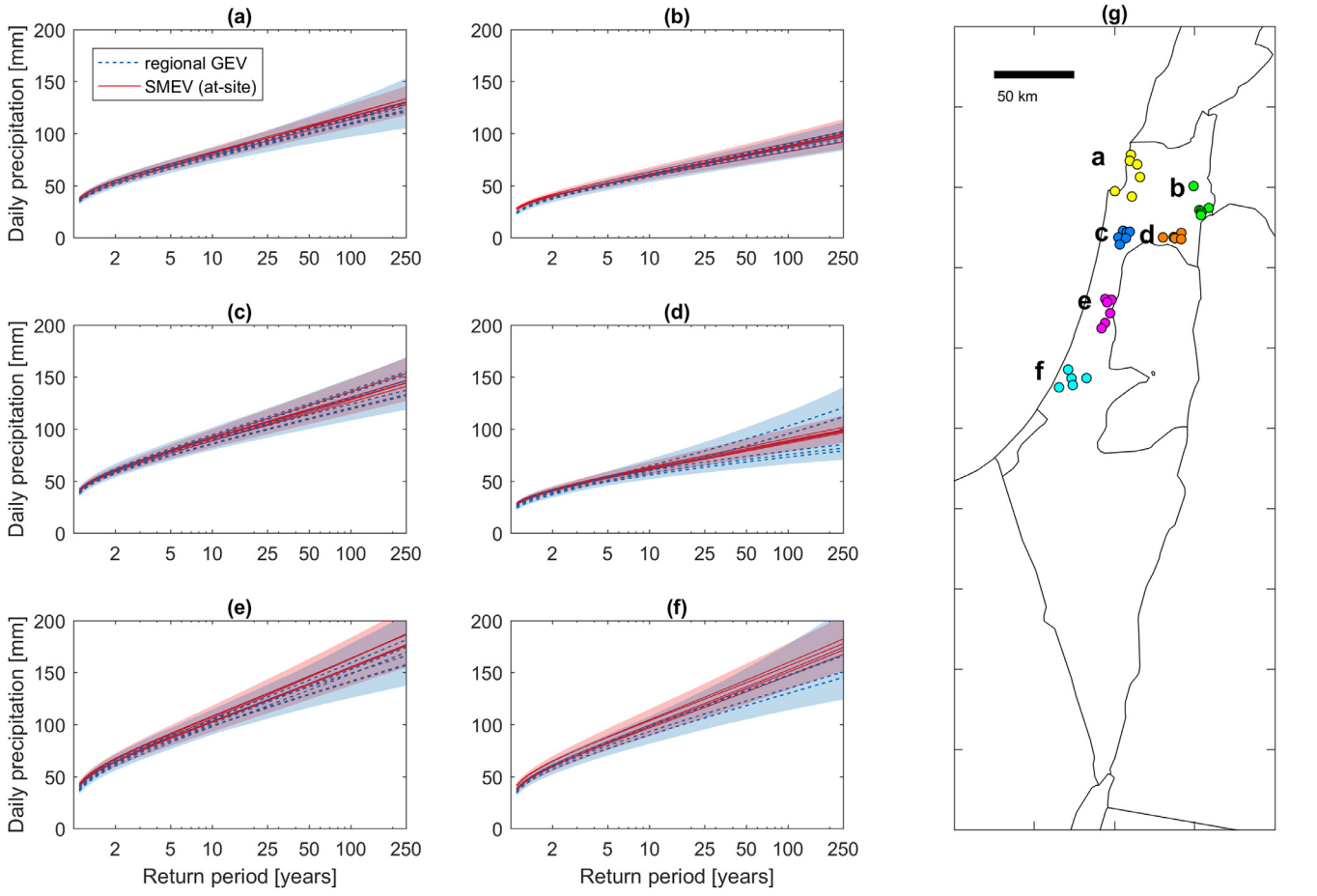


**Fig. 4.** (a-f) Graphical comparison of daily precipitation quantiles obtained using the proposed SMEV formulation (red lines, at-site application) and a regional GEV approach (blue dashed lines) for a set of homogeneous regions whose geographic location is shown in (g). Shaded areas represent the compound 90% confidence interval for the stations in each region. (For interpretation of the references to colour in this figure legend, the reader is referred to the web version of this article.)

The spatial consistency of the parameters indirectly provides a positive feedback on the meaningfulness of the approach. The spatial patterns in Fig. 2b, c, e, f, h, i suggest that the width of the distributions in Fig. 2a, d, g is caused by the fact that wide areas characterized by different climatic characteristics are examined, rather than by uncertainty in the parameters estimation alone. The strong North to South gradient in the number of yearly occurrences (Fig. 2h, i) and in the Weibull scale parameters (Fig. 2b, c) reflects the climatology of the area. The shape parameters show lower values (i.e., heavier-tailed distributions) in the coastal region and in the arid areas, particularly for the Type 1–Lows, confirming prior knowledge about the climatology of extreme precipitation in drylands in general (Nicholson, 2011), and in the eastern Mediterranean in particular (Goldreich 2012; Marra et al., 2017). Such a spatial consistency suggests applicability of the method in the identification of homogeneous regions within regionalization frameworks, as well as spatial interpolation of the parameters to derive distributed maps of high quantiles.

Fig. 4 shows the frequency curves and relative uncertainty obtained over homogeneous regions using the SMEV method on individual stations (at-site) and the regionalized GEV framework in each region. Despite the at-site application, the SMEV method allows estimates of large quantiles characterized by large spatial consistency among nearby homogeneous stations and generally reduced uncertainty with respect to regional GEV estimates. This supports the use of ordinary events to model extreme precipitation, confirming previous studies by Marani and Ignaccolo (2015), Zorzetto et al. (2016), and Marra et al. (2018).

### 3.5. Sensitivity analysis to changes in the parameters

We explore here the effects of changes in ordinary rainfall regimes on extreme precipitation by exploiting how the MEV approach separates the role of the distribution of ordinary rainfall intensity and of the number of events per year and the simplified formulation provided by SMEV. Empirical observation of the data shows that the scale and shape parameters of the Weibull distributions describing the two synoptic classes in the region are related to each other (Fig. 5). Increases in the scale parameter are likely to be associated to increases in the shape parameter, and a linear model can provide a first approximation of such relation (Fig. 5).

The sensitivity of the 100-year quantiles to changes in the ordinary events intensity (following the linear relations between the parameters shown in Fig. 4) and in the number of yearly occurrences around typical values observed in the area is shown in Fig. 6. Black dots in the figure represent the typical observed conditions ($\lambda_{Lows} = 11.7$, $\kappa_{Lows} = 0.90$, $\lambda_{Lows} = 30.5$, $\lambda_{Other} = 4.11$, $\kappa_{Other} = 0.70$, $n_{Other} = 17.9$). Although Fig. 6 shows the sensitivity of the 100-year quantiles to changes in the SMEV parameters, any other quantile can be reproduced, and site-specific figures with the exact parameters of the location of interest can be easily drawn. The approach can be used to (a) quantify the impact of changes in the intensity and number of yearly occurrences of rainy days generated by each synoptic class, as well as (b) understand the uncertainty levels to be associated to uncertainty in the estimated parameters. For instance, Fig. 6b shows that changes/uncertainty in the intensity of the Type 1–Lows are expected to affect the 100-year

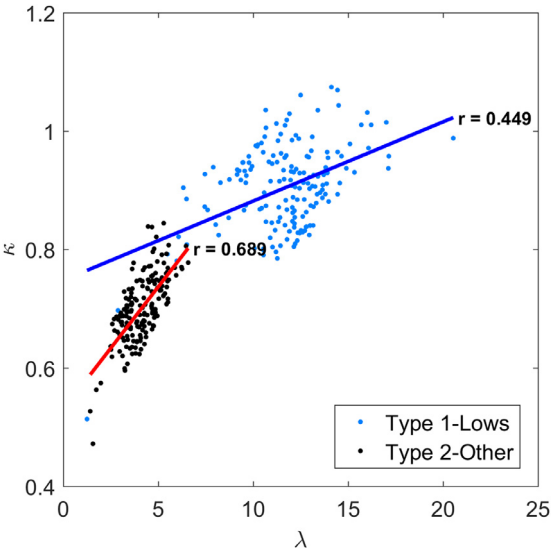


**Fig. 5.** Empirical relation between scale ($\lambda$) and shape ($\kappa$) parameters of the Weibull distributions describing the two synoptic classes.

quantiles more than changes/uncertainty in the intensity of the Type 2–Other class, but, should the intensity of the two classes become comparable, changes of both would be expected to impact. At the same time, Fig. 6c shows that the intensity of the Type 1–Lows dominates over their number of yearly occurrences, unless this number decreases to less than ~10 events per year.

### 3.6. Modeling temporal changes in the climatic conditions

An example of application of the framework using future projections of the parameters is presented in Fig. 7, where the response of high quantiles (2- to 100-year quantiles) to reasonable temporal changes in the intensity and occurrence of the Type 1–Lows are simulated. Specifically, initial conditions typical of the observations are parametrized ($\lambda_{Lows} = 11.7$, $\kappa_{Lows} = 0.9$, $n_{Lows} = 30.5$) and then (a) a 2 °C increase in temperature (IPCC, 2014), and (b) a 22% decrease in the average number of yearly Type 1–Lows (Hochman et al., 2018a, RCP4.5 scenario), both occurring linearly over an 80-year period, are simulated. Changes in the ordinary events intensity is simulated assuming a 3.5%/°C scaling of the median intensities with temperature (Peleg et al., 2018a) and following the linear relation between scale and shape parameter shown in Fig. 5. Intensity and frequency of the Type 2–Other events are kept constant ($\lambda_{Other} = 4.11$, $\kappa_{Other} = 0.7$, $n_{Other} = 17.9$).

The factors of change resulting from this example strongly depend on the quantile of interest, with 100-year quantiles showing an increase up to ~1% and 2-year and 10-year quantiles observing an overall decrease of ~2% and ~1%, respectively (Fig. 7a). The response of the 25-year quantiles, also reported in Fig. 7b, shows a complex behavior, with a slight increase during the first ~40 years and a decrease back to its initial value after 80 years.

It should be pointed out that Figs. 6 and 7 only show illustrative applications of the framework. Before extracting quantitative information

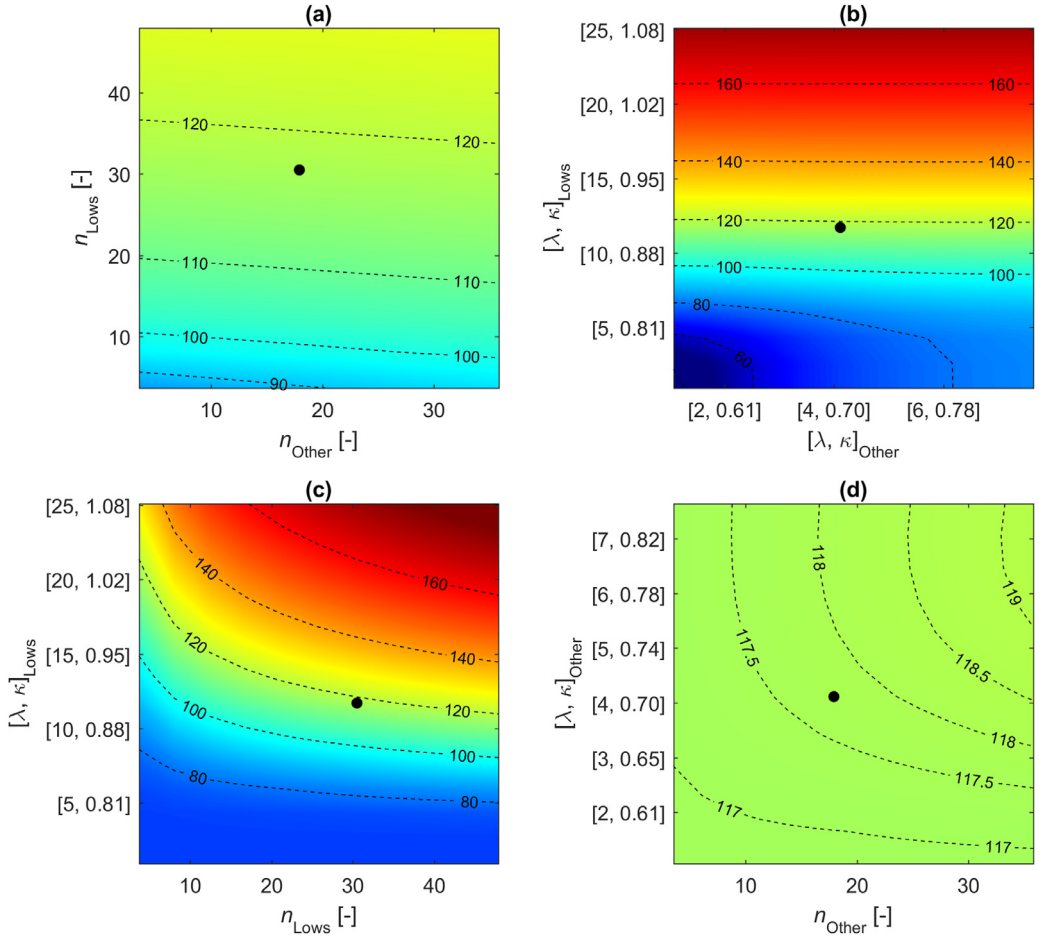


**Fig. 6.** Sensitivity of the 100-year quantiles (colors and contours) to changes in intensity (following the empirical relations between scale ($\lambda$) and shape ($\kappa$) parameters shown in Fig. 5) and number of yearly occurrences ($n$) of the two synoptic classes for typical values of the parameters. Black dots show the typical observed values.

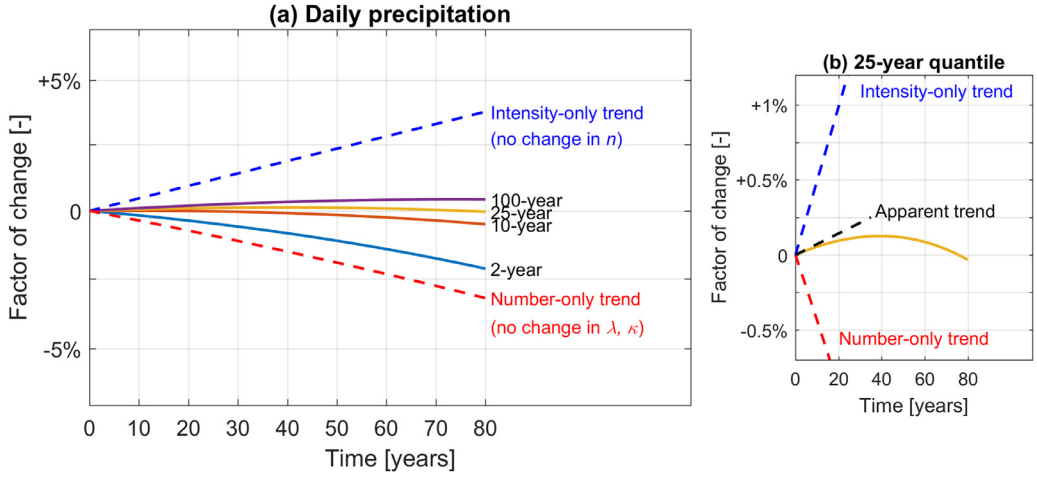


**Fig. 7.** (a) Modelled variations of the 2-, 10-, 25- and 100-year quantiles under changes in the intensity of the Type 1–Lows, i.e. +3.5%/°C in the median intensities (Peleg et al., 2018a), +2 °C in 80 years (IPCC, 2014) and yearly occurrences, i.e. −22% in 80 years (Hochman et al., 2018a). Parameters and occurrences of Type 2–Other events are kept constant. (b) Zoom on the 25-year quantiles.

from such analyses, one should consider possible correlations among the parameters and, if relevant, include them in the formulation; for instance, in the examined region, correlation between the number of occurrences of the two synoptic classes is expected.

## 4. Discussion

### 4.1. Modeling multiple underlying processes

The synoptic classification used in this study constitutes an example case and, in other regions of the world, precipitation extremes may emerge from different types of generating mechanisms (e.g., winter/summer precipitation, tropical/typical storms, etc.).

Despite one of the synoptic classes being greater in intensity and number of occurrences, both classes may contribute to the observed extreme daily amounts (e.g., Fig. 3, confirmed by most of the analyzed stations). The i/id assumption of extreme value theory is thus violated even if one is only interested in the upper tail of the distribution. Interestingly, the upper tail of a mixture of Weibull distributions characterized by similar enough parameters is almost Weibull distributed, at least within the sampling uncertainties characterizing real datasets (see Fig. 8a, recalling that, using the transformation in the figure, Weibull distributions are linear). Conversely, in presence of increasingly different parameter sets, particularly the shape parameter, the upper tail (Fig. 8b) or the entire compound distribution (Fig. 8c) may diverge from a Weibull behavior (Elmahdy and Aboutahoun, 2013). Presence of processes characterized by Weibull distributions with similar shape parameter explains the goodness of the Weibull model for the upper tail reported by previous studies (Marani and Ignaccolo, 2015; Zorzetto et al., 2016; Marra et al., 2018; Papalexiou et al., 2018) as well as the goodness of the Weibull models used in this study to represent synoptic classes grouping different synoptic types together. The presence of multiple types of ordinary events that are sampled with varying proportions each year may contribute to the inter-annual variability of the Weibull parameters observed in previous studies which considered a single type of ordinary events (Marani and Ignaccolo, 2015; Zorzetto et al., 2016). However, a single-event-type formulation would not allow to model individual changes in the occurrences of the different types, as the parameters derived for the mixed distribution depend both on the parameters of the individual distributions and on the mixing proportion (Woodward and Gunst, 1987).

Comparing quantiles derived using the here-proposed SMEV formulation and a classic regional GEV approach (Fig. 4) shows that at-site SMEV estimates are extremely consistent in space and generally characterized by decreased uncertainty. This suggests that ordinary events can provide accurate information on the upper tail, and supports the results obtained from multifractal theory by Veneziano et al. (2009). The parameters representing the upper tail of the distribution can be successfully computed using 25% of the data, with significant advantages in terms of data sample and fit accuracy. The results by Marra et al. (2018),

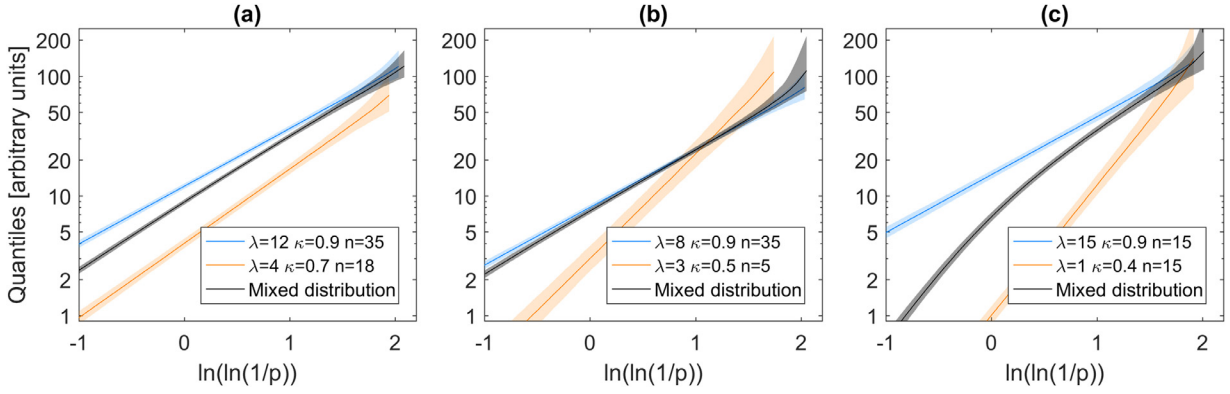


**Fig. 8.** Mixtures of Weibull distributions for three example cases. Samples from 1000 repetitions of 60-year records. Solid lines show the median value, shaded areas the 90% sampling uncertainty. (a) Mixture of Weibull distributions with characteristics similar to the ones describing the two examined synoptic classes (e.g., Fig. 2). (b, c) Mixture of Weibull distributions with increasingly different parameters sets.

who quantified the impact of measurement errors on frequency analyses from extreme value theory and MEV, provide additional support to the robustness of the formulation. Due to the limited data sample, extracting the parameters from the upper tail alone, as done in classic extreme value theory approaches, provides estimates characterized by comparable uncertainty even within regionalization approaches based on individual records exceeding 60 years (at this regard, see also Willems (2013) and Peleg et al. (2018b)).

### 4.3. Modeling changing conditions

The presented method allows to easily quantify the probability of exceedance of extreme quantiles emerging from multiple underlying processes. For the case of daily precipitation, the formulation makes use of three parameters for each type of underlying process, with one of the parameters being the average number of yearly occurrences, i.e. the probability of occurrence of an ordinary event. This represents an important improvement with respect to classic extreme value formulations, in which the same number of parameters is usually required, but the connection with the physical processes generating the extremes is indirect.

Fig. 7 shows the combination of projected changes in the yearly occurrences of Mediterranean lows (Hochmann et al., 2018a) and scaling of the median events intensity with temperature (Peleg et al., 2018a) for the eastern Mediterranean. The obtained response is very instructive, and shows how the presence of very simple trends in intensity (linear temperature increase, exponential temperature-intensity scaling) and number of yearly occurrences (linear decrease) may lead to complicated responses in the extreme quantiles. As already pointed out by Montanari and Koutsoyiannis (2014) and Koutsoyiannis and Montanari (2015), among others, extrapolating trends directly from observations of the target processes (e.g., Ganguli et al., 2017; Serago and Vogel, 2018) may lead to misleading results (e.g., the black dashed line in Fig. 7b).

Modeling changing climatic conditions often makes use of global or regional reanalyses and/or climate models (e.g., Ragno et al., 2018), which are generally characterized by coarse resolutions and conditional biases. Downscaling models can be used to reproduce the required resolutions (e.g., So et al., 2017), but strong assumptions on the scale-independence of the factors of change need to be adopted. SMEV allows to independently treat temporal changes in the processes intensities (e.g., Contractor et al., 2018) and on their yearly occurrences, which, owing to the larger amount of ordinary (versus extreme) events, can be derived in an easier way from observations, reanalyses or climate models (e.g., Peleg et al., 2015b; Ragno et al., 2018; Marelle et al., 2018). This can be done with the purpose of (a) modeling future extremes under assumptions of deterministic changes in these components (e.g., Fig. 7), (b) investigating temporal changes in past observations, or (c) modeling past nonstationary conditions (e.g., seasonality, influence of climatic indices). In addition, the model allows to (d) parsimoniously quantify the sensitivity of extreme quantiles to any change in intensity and yearly occurrences of the underlying processes (e.g., Fig. 6). The extremely limited computational demand required by SMEV allows stochastic applications, which may help understanding how uncertainty in the modelled changes propagate to the target processes, and use in combination with ensemble climate models and/or reanalyses.

## 5. Conclusions

A new Simplified Metastatistical Extreme Value (SMEV) formulation for the analysis of hydro-meteorological extremes emerging from multiple underlying processes is provided. SMEV describes extremes by means of parameters directly related to the average properties of the ordinary events, such as intensity and average number of yearly occurrences.

The method is applied to extreme daily precipitation using Weibull distributions to model the daily precipitation amounts generated by two classes of synoptic systems. This provides an extreme value distribution described by three parameters for each class: two parameters describing the events intensity, and one related to their probability of occurrence. Both the classes are observed to contribute extreme daily amounts and distinct parameters sets are required to describe the respective ordinary events, meaning that the identical distribution assumption of extreme value theory is violated even when focusing on the upper tail of the distribution. SMEV provides extreme quantiles which are highly consistent among stations in homogenous regions and, despite the at-site application, generally characterized by reduced uncertainty with respect to classic regional GEV frameworks. Simple combinations of trends in the intensity and yearly occurrences of the processes leads to rather complicated responses in the extremes so that extrapolating trends directly from observations of the target process may lead to largely misleading conclusions.

SMEV provides a robust framework for frequency analyses of extremes emerging from multiple underlying processes, and represents a parsimonious tool for computationally efficient sensitivity analyses, explanatory models, nonstationary frequency analyses, and climate projections.

## Data availability

Daily precipitation data used in this study were provided by the Israel Meteorological Service (www.ims.gov.il) in July 2018.

## Competing interests

The authors declare no conflict of interest.

## Acknowledgments

This study was funded by the Israel Ministry of Science and Technology [grant no. 61792], the Israel Science Foundation [grant no. 1069/18], by NSF-BSF grant [BSF 2016953], and by a Google gift grant. This study is a contribution to the PALEX project “Paleohydrology and Extreme Floods from the Dead Sea ICDP Core” funded by the DFG [BR2208/13-1/-2], and is a contribution to the HyMeX program. The authors would like to thank Prof. Pinhas Alpert for providing the updated synoptic classification. Comments from the editor Simon Michael Papalexiou and three anonymous reviewers greatly helped improving this study.

## Supplementary materials

Supplementary material associated with this article can be found, in the online version, at doi:10.1016/j.advwatres.2019.04.002.

## References

Alpert, P., Ben-Gai, T., Baharad, A., Benjamini, Y., Yekutieli, D., Colacino, M., Diodato, L., Ramis, C., Homar, V., Romero, R., Michaelides, S., Manes, A., 2002. The paradoxical increase of mediterranean extreme daily rainfall in spite of decrease in total values. Geophys. Res. Lett. 29 (11), 31. http://doi.org/10.1029/2001GL013554.

Alpert, P., Osetinsky, I., Ziv, B., Shafir, H., 2004. Semi-objective classification for daily synoptic systems: application to the Eastern Mediterranean climate change. Int. J. Climatol. 24 (8), 1001–1011. https://doi.org/10.1002/joc.1036.

Agilan, V., Umamahesh, N.V., 2017. Non-stationary rainfall intensity-duration-frequency relationship: a comparison between annual maximum and partial duration series. Water Resour. Manage. 31, 1825–1841. https://doi.org/10.1007/s11269-017-1614-9.

Armon, M., Dente, E., Smith, J.A., Enzel, Y., Morin, E., 2018. Synoptic-scale control over modern rainfall and flood patterns in the levant drylands with implications for past climates. J. Hydrometeorol. 19, 1077–1096. https://doi.org/10.1175/JHM-D-18-0013.s1.

Atlas of Israel, 1970. Cartography, Physical Geography, Human and Economical Geography, History. Survey of Israel. Min. of Labour, Jerusalem, and Elsevier, Amsterdam, 1970 Ca, p. 300. pages.

Belachsen, I., Marra, F., Peleg, N., Morin, E., 2017. Convective rainfall in a dry climate: relations with synoptic systems and flash-flood generation in the Dead Sea region. Hydrol. Earth Syst. Sci. 21, 5165–5180. https://doi.org/10.5194/hess-21-5165-2017.

Berg, P., Moseley, C., Haerter, J.O., 2013. Strong increase in convective precipitation in response to higher temperatures. Nat. Geosci. 6 (3), 181–185. https://doi.org/10.1038/ngeo1731.

Cheng, L., AghaKouchak, A., 2014. Nonstationary precipitation intensity-duration-frequency curves for infrastructure design in a changing climate. Sci. Rep. 4, 7093. https://doi.org/10.1038/srep07093.

Contractor, S., Donat, M.G., Alexander, L.V., 2018. Intensification of the daily wet day rainfall distribution across Australia. Geophys. Res. Lett. 45. https://doi.org/10.1029/2018GL078875.

Dayan, U., Morin, E., 2006. Flash flood – producing rainstorms over the Dead Seas: a review. New Front. Deas Seas Paleoenviron. *Re*. Geol. Soc. Am. Spec. Pap. 401, 53–62. https://doi.org/10.1130/2006.2401(04).

Dobrinski, P., Da Silva, N., Panthou, G., Bastin, S., Muller, C., Ahrens, B., Borga, M., Conte, D., Fosser, G., Giorgi, F., Guttler, I., Kotroni, V., Li, L., Morin, E., Onol, B., Quintana-Segui, P., Romera, R., Torma, C.Z., 2016. Scaling precipitation extremes with temperature in the Mediterranean: past climate assessment and projection in anthropogenic scenarios. Clim. Dyn. 1–21. https://doi.org/10.1007/s00382-016-3083-x.

Elmahdy, E.E., Aboutahoun, A.W., 2013. A new approach for parameter estimation of finite weibull mixture distributions for reliability modeling. Appl. Math. Model. 37 (4), 1800–1810. http://doi.org/10.1016/j.apm.2012.04.023.

Fischer, S., 2018. A seasonal mixed-POT model to estimate high flood quantiles from different event types and seasons. J. Appl. Stat. https://doi.org/10.1080/02664763.2018.1441385.

Fischer, E.M., Knutti, R., 2016. Observed heavy precipitation increase confirms theory and early models. Nat Clim Change 6 (11), 986–991. https://doi.org/10.1038/NCLIMATE3110.

Fischer, R., Tippett, L., 1928. Limiting forms of the frequency distribution of the largest or smallest member of a sample. Math. Proc. Cambridge 24, 180–190.

Ganguli, P., Coulibaly, P., 2017. Does nonstationarity in rainfall require nonstationary intensity–duration–frequency curves? Hydrol. Earth Syst. Sci. 21, 6461–6483. https://doi.org/10.5194/hess-21-6461-2017.

Goldreich, 2012. The Climate of Israel: Observation. In: Research and Application. Springer, p. 270.

Gnedenko, B., 1943. Sur la distribution limite du terme maximum d'une serie aleatoire. Ann. Math. 44, 423–453.

Hardwick Jones, R., Westra, S., Sharma, A., 2010. Observed relationships between extreme sub-daily precipitation, surface temperature, and relative humidity. Geophys. Res. Lett. 37. https://doi.org/10.1029/2010GL045081.

Hall, J., Arheimer, B., Borga, M., Brázdil, R., Claps, P., Kiss, A., Kjeldsen, T.R., Kriaučiūnienė, J., Kundzewicz, Z.W., Lang, M., M.C., Llasat, Macdonald, N., McIntyre, N., Mediero, L., Merz, B., Merz, R., Molnar, P., Montanari, A., Neuhold, C., Parajka, J., Perdigão, R.A.P., Plavcová, L., Rogger, M., Salinas, J.L., Sauquet, E., Schär, C., Szolgay, J., Viglione, A., Blöschl, G., 2014. Understanding flood regime changes in Europe: A state-of-the-art assessment. Hydrol. Earth Syst. Sci. 18, 2735–2772. https://doi.org/10.5194/hess-18-2735-2014.

Hirschboeck, K.K., 1987. Hydroclimatically-defined mixed distributions in partial duration flood series, in: Singh, V.P. (Ed). In: Hydrologic Frequency Modeling: Proceedings of the International Symposium on Flood Frequency and Risk Analyses, 14-17 May 1986, Louisiana State University, Baton Rouge, U.S.A.,. Springer Netherlands, Dordrecht, pp. 199–212. https://doi.org/10.1007/978-94-009-3953-0_13.

Hochman, A., Harpaz, T., Saaronia, H., Alpert, P., 2018a. Synoptic classification in 21st century CMIP5 predictions over the Eastern Mediterranean with focus on cyclones. Int. J. Climatol 38, 1476–1483. https://doi.org/10.1002/joc.5260.

Hochman, A., Mercogliano, P., Alpert, P., Saaroni, H., Bucchignani, E., 2018b. High-resolution projection of climate change and extremity over Israel using COSMO-CLM. Int. J. Climatol 1–12. http://doi.org/10.1002/joc.5714.

Hosking, J.R.M., Wallis, J.R., 1997. Regional Frequency Analysis: An Approach Based on L-moments. Cambridge University Press, UK. http://dx.doi.org/10.1017/cbo9780511529443.

Iliopoulou, T., Koutsoyiannis, D., Montanari, A., 2018. Characterizing and modeling seasonality in extreme rainfall. Water Resour. Res. 54. https://doi.org/10.1029/2018WR023360.

IPCC, 2014. Climate Change 2014: synthesis Report. In: Pachauri, R.K., Meyer, L.A. (Eds.), Contribution of Working Groups I, II and III to the Fifth Assessment Report of the Intergovernmental Panel On Climate Change [Core Writing Team]. IPCC, Geneva, Switzerland, p. 151.

Kendon, E.J., Ban, N., Roberts, N.M., Fowler, H.J., Roberts, M.J., Chan, S.C., Evans, J.P., Fosser, G., Wilkinson, J.M, 2017. Do convection-permitting regional climate models improve projections of future precipitation change? Bull. Am. Meteorol. Soc. 98 (1), 79–93. https://doi.org/10.1175/BAMS-D-15-0004.2.

Khaliq, M.N., Ouarda, T.B.M.J., Ondo, J.C., Gachon, P., Bobée, B., 2006. Frequency analysis of a sequence of dependent and/or non-stationary hydro-meteorological observations: a review. J. Hydrol 329 (3–4), 534–552. https://doi.org/10.1016/j.jhydrol.2006.03.004.

Koutsoyiannis, D., Montanari, A., 2015. Negligent killing of scientific concepts: the stationarity case. Hydrol. Sci. J. 60 (7–8), 1174–1183. https://doi.org/10.1080/02626667.2014.959959.

Lepore, C., Veneziano, D., Molini, A., 2015. Temperature and CAPE dependence of rainfall extremes in the eastern United States. Geophys. Res. Lett. 42 (1), 74–83. https://doi.org/10.1002/2014GL062247.

Marani, M., Ignaccolo, M., 2015. A metastatistical approach to rainfall extremes. Adv. Water Resour. 79, 121–126. https://doi.org/10.1016/j.advwatres.2015.03.001.

Marelle, L., Myhre, G., Hodnebrog, Ø., Sillmann, J., Samset, B.H., 2018. The changing seasonality of extreme daily precipitation. Geophys. Res. Lett. 45. https://doi.org/10.1029/2018GL079567.

Marra, F., Morin, E., Peleg, N., Mei, Y., Anagnostou, E.N., 2017. Intensity–duration–frequency curves from remote sensing rainfall estimates: comparing satellite and weather radar over the eastern Mediterranean. Hydrol. Earth Syst. Sci. 21, 2389–2404. https://doi.org/10.5194/hess-21-2389-2017.

Marra, F., Nikolopoulos, E.I., Anagnostou, E.N., Morin, E., 2018. Metastatistical extreme value analysis of hourly rainfall from short records: estimation of high quantiles and impact of measurement errors. Adv. Water Resour. 117, 27–39. https://doi.org/10.1016/j.advwatres.2018.05.001.

Meresa, H.K., Romanowicz, R.J., 2017. The critical role of uncertainty in projections of hydrological extremes. Hydrol. Earth Syst. Sci. 21, 4245–4258. https://doi.org/10.5194/hess-21-4245-2017.

Montanari, A., Koutsoyiannis, D., 2014. Modeling and mitigating natural hazards: stationary is immortal. Water Resour. Res. 50, 9748–9756. https://doi.org/10.1002/2014WR016092.

Morin, E., 2011. To know what we cannot know: global mapping of minimal detectable absolute trends in annual precipitation. Water Resour. Res. 47 (7), 1–9. https://doi.org/10.1029/2010WR009798.

Nicholson, S.E., 2011. Dryland Climatology. Cambridge University Press, Cambridge https://doi.org/10.1017/CBO9780511973840.

Overeem, Aart, Buishand, Adri, Holleman, Iwan, 2008. Rainfall depth-duration- frequency curves and their uncertainties. J. Hydrol. 348 (1–2), 124–134. https://doi.org/10.1016/j.jhydrol.2007.09.044.

Papalexiou, S.M., AghaKouchak, A., Foufoula-Georgiou, E., 2018. A diagnostic framework for understanding climatology of tails of hourly precipitation extremes in the United States. Water Resour. Res. 54. https://doi.org/10.1029/2018WR022732.

Peleg, N., Bartov, M., Morin, E., 2015a. CMIP5-Predicted climate shifts over the east mediterranean: implications for the transition region between mediterranean and semi-arid climates. Int. J. Climatol. 35 (8), 2144–2153. https://doi.org/10.1002/joc.4114.

Peleg, N., Shamir, E., Georgakakos, K.P., Morin, E., 2015b. A framework for assessing hydrological regime sensitivity to climate change in a convective rainfall environment: a case study of two medium-sized eastern Mediterranean catchments. Israel. Hydrol. Earth Syst. Sci. 19, 567–581. https://doi.org/10.5194/hess-19-567-2015.

Peleg, N., Marra, F., Fatichi, S., Molnar, P., Morin, E., Sharma, A., Burlando, P., 2018a. Intensification of convective rain cells at warmer temperatures observed from high-resolution weather radar data. J. Hydrometeor. 19, 715–726. https://doi.org/10.1175/JHM-D-17-0158.1.

Peleg, N., Marra, F., Fatichi, S., Paschalis, A., Molnar, P., Burlando, P., 2018b. Spatial variability of extreme rainfall at radar subpixel scale. J. Hydrol. 556, 922–933. http://doi.org/10.1016/j.jhydrol.2016.05.033.

Pineda, L.E., Willems, P., 2018. Rainfall extremes, weather and climate drivers in complex terrain: a data-driven approach based on signal enhancement methods and EV modeling. J. Hydrol 563, 283–302. https://doi.org/10.1016/j.jhydrol.2018.05.062.

Ragno, E., AghaKouchak, A., Love, C.A., Cheng, L., Vahedifard, F., Lima, C.H.R., 2018. Quantifying changes in future intensity-duration-frequency curves using multimodel ensemble simulations. Water Resour. Res. 54. https://doi.org/10.1002/2017WR021975.

Serago, J.M., Vogel, R.M., 2018. Parsimonious nonstationary flood frequency analysis. Adv. Water Resour. 112, 1–16. https://doi.org/10.1016/j.advwatres.2017.11.026.

Serinaldi, F., Kilsby, C.G., 2015. Stationarity is undead: uncertainty dominates the distribution of extremes. Adv. Water. Resour. 77, 17–36. https://doi.org/10.1016/j.advwatres.2014.12.013.

Serinaldi, F., Kilsby, C.G., 2018. Unsurprising surprises: the frequency of record-breaking and over-threshold hydrological extremes under spatial and temporal dependence. Water Resour. Res. https://doi.org/10.1029/2018WR023055.

Serinaldi, F., Kilsby, C.G., Lombardo, F., 2018. Untenable nonstationarity: an assessment of the fitness for purpose of trend tests in hydrology. Adv. Water Res. 111, 132–155. https://doi.org/10.1016/j.advwatres.2017.10.015.

So, B.-J., Kim, J.-Y., Kwon, H.-H., Lima, C.H.R., 2017. Stochastic extreme downscaling model for an assessment of changes in rainfall intensity-duration-frequency curves over South Korea using multiple regional climate models. J. Hydrol. 553, 321–337. http://dx.doi.org/10.1016/j.jhydrol.2017.07.061.

Sun, X., Thyer, M., Renard, B., Lang, M., 2014. A general regional frequency analysis framework for quantifying local-scale climate effects: a case study of ENSO effects on Southeast Queensland rainfall. J. Hydrol 512, 53–68. https://doi.org/10.1016/j.jhydrol.2014.02.025.

Tabari, H., Willems, P., 2018. More prolonged droughts by the end of the century in the Middle East. Environ. Res. Lett. in press https://doi.org/10.1088/1748-9326/aae09c.

Veneziano, D., Langousis, A., Lepore, C., 2009. New asymptotic and preasymptotic results on rainfall maxima from multifractal theory. Water Resour. Res. 45, W11421. https://doi.org/10.1029/2009WR008257.

Villarini, G., Serinaldi, F., Smith, J.A., Krajewski, W.F., 2009. On the stationarity of annual flood peaks in the continental United States during the 20th century. Water Resour. Res. 45, W08417. https://doi.org/10.1029/2008WR007645.

de Vries, A.J., Tyrlis, E., Edry, D., Krichak, S.O., Steil, B., Lelieveld, J., 2013. Extreme precipitation events in the Middle East: dynamics of the Active Red Sea Trough. J. Geophys. Res. Atmos. 118, 7087–7108. http://doi.org/10.1002/jgrd.50569.

Wasko, C., Parinussa, R.M., Sharma, A., 2016. A quasi-global assessment of changes in remotely sensed rainfall extremes with temperature. Geophys. Res. Lett. 43 (12), 12. 659–668 http://doi.org/10.1002/2016GL071354 .

Weibull, W., 1951. A statistical distribution of wide applicability. J. Appl. Mech. 18, 239–296.

Westra, S., Alexander, L., Zwiers, F., 2013. Global increasing trends in annual maximum daily precipitation. J. Clim 26, 3904–3918. https://doi.org/10.1175/JCLI-D-12-00502.1.

Westra, S., Fowler, H.J., J.P.Evans, L.V.Alexander, Berg, P., Johnson, F., Kendon, E.J., Lenderink, G., Roberts, N.M., 2014. Future changes to the intensity and frequency of short-duration extreme rainfall. Rev. Geophys. 52 (3), 522–555. https://doi.org/10.1002/2014RG000464.

Willems, P., 2000. Compound Intensity/duration/frequency-relationships of extreme precipitation for two seasons and two storm types. J. Hydrol. 233, 189–205. https://doi.org/10.1016/S0022-1694(00)00233-X.

Willems, P., 2013. Adjustment of extreme rainfall statistics accounting for multi-decadal climate oscillations. J. Hydrol. 490, 126–133. http://doi.org/10.1016/j.jhydrol.2013.03.034.

Wilson, P., Tuomi, R., 2005. A fundamental probability distribution for heavy rainfall. Geophys. Res. Lett. 32, L14812. https://doi.org/10.1029/2005GL022465.

Woodward, Wayne A., Gunst, Richard F., 1987. Using mixtures of Weibull distributions to estimate mixing proportions. Comp. Stat. Data Analysis 5 (3), 163–176. https://doi.org/10.1016/0167-9473(87)90012-0.

Yarnal, B., 1993. Synoptic Climatology in Environmental analysis: A primer. Belhaven Press, London.

Ziv, B., H. Saaroni, T. Harpaz, P. Alpert, 2010. Trends in rainfall regime over Israel, 1975–2010, and their relationship to large-scale variability. https://doi.org/10.1007/s10113-013-0414-x.

Zorzetto, E., Botter, G., Marani, M., 2016. On the emergence of rainfall extremes from ordinary events. Geophys. Res. Lett. 43, 8076–8082. https://doi.org/10.1002/2016GL069445.